ADVANCED OPTICAL MATERIALS
www.advopticalmat.de

Single Plasmonic Oligomer Chiral Spectroscopy

Julian Karst, Nikolai Strohfeldt, Martin Schäferling, Harald Giessen, and Mario Hentschel*

Chirality plays a crucial role in our everyday lives. Many biomolecules are handed and the associated biological processes rely on their handedness. Thus, chirality is investigated intensely, also because of the fundamental and inherent interest in the concept of chirality. However, virtually all studies are performed on large ensembles of chiral objects, which obstructs the contribution of the individual particle. Hence, it is highly desirable to study individual chiral objects. Here, it is shown how to measure chiroptical spectra in the visible spectral range of left- and right-handed C_4 symmetric single plasmonic nanoantenna ensembles, which are termed oligomers. The two-layered oligomers are fabricated by top-down electron beam lithography to offer a high degree of structural control. Dark-field scattering spectroscopy as well as correlative scanning electron microscopy are utilized to study the influence of structural arrangement and individual shape on the optical properties of a single plasmonic oligomer. Even minute structural differences, which cannot be resolved in scanning electron microscopy, manifest themselves in clear differences in the chiroptical response. The results play an important role for further investigations and optimizations in design, fabrication, and measurements of single plasmonic enantiomers but also on the way toward single chiral object sensing.

1. Introduction

Chirality is one of the most prominent principles in nature. Among the fundamental building blocks of living matter are proteins and nucleic acids as the carrier of genetic information. Both contain handed structures. Proteins are interlinked amino acids whereas nucleic acids consist of nucleotides, of which both classes feature right- or left-handed entities.

A significant amount of scientific research is consequently devoted to chiral objects. The interest in chirality is not limited to chemistry and biology but also extends to physics. Apart from distinct molecular interactions between handed molecules, chirality can also manifest itself optically.[1,2] This chiroptical response is in fact the most straightforward way to analyze and study chiral systems. Chiral objects show different absorption of left- and right-handed circularly polarized light, which is called circular dichroism (CD). Solutions of chiral molecules are also able to rotate the plane of incident linearly polarized light depending on their respective handedness, the so-called optical rotatory dispersion. In general, these two quantities are Kramers–Kronig related.[3] Both effects can be utilized to study chiral molecules, with circular dichroism spectroscopy being the most commonly used. Chirality is a powerful method to analyze the 3D conformation of molecules as it is an intrinsically 3D property. CD spectra can help to unravel the secondary structure of proteins, which is ultimately responsible for the interaction of proteins and for the biologically and physiologically relevant processes.[4] That said, it is obvious that the exact conformation of a molecule and the differences between the molecules of an ensemble are of paramount interest. However, in chemistry and biology the CD of many molecules is measured in a solution with a CD spectrometer, as the CD response of a single molecule appears to be too small to be determined. This measurement scheme obstructs the contribution of the individual molecule and thus does not allow for single molecule based secondary structure investigations.

In recent years, researchers have been intensely studying chiral plasmonic systems.[5–12] A plasmon is the collective oscillation of the quasi-free conduction electrons in a metallic nanoparticle. Such plasmon resonances have large resonant light interaction cross sections which allow for the detection and measurement of single nanostructures. What is more, the locally enhanced near-fields associated with the plasmon resonance allow to couple adjacent nanoparticles and create plasmonic molecules of nearly arbitrary complexity. Due to advances in the top-down techniques related to micro- and nanofabrication, we are able to structure such systems in two and three dimensions nearly at will.[13–15] Additionally, bottom-up techniques, such as DNA-mediated self-assembly,[16–20] even allow for switchable chiral structures.[21–28] Two aspects are of particular importance here: On the one hand, the tunability of these systems allows studying the properties of chirality in great detail while having full control over the chiral plasmonic structures,[29,30] which is in stark contrast to molecular systems whose structures cannot be manipulated easily. On the other hand, researchers are searching for interactions between chiral (bio)-molecules and chiral plasmonic molecules which could lead to decreased detection limits.[31–36]

In all the mentioned cases, it is of large interest to study single structures and unravel the influence of even minute conformational differences or to track changes in time on a single structure level. Dark-field scattering spectroscopy has been widely used to measure the (chiral) optical response of single

J. Karst, Dr. N. Strohfeldt, Dr. M. Schäferling, Prof. H. Giessen, Dr. M. Hentschel
4th Physics Institute and Research Center SCoPE
University of Stuttgart
Pfaffenwaldring 57, 70569 Stuttgart, Germany
E-mail: h.giessen@pi4.uni-stuttgart.de

DOI: 10.1002/adom.201800087

plasmonic molecules or particles,[37–40] such as extrinsically chiral systems,[41] self-assembled 3D structures,[42,43] or lithographically prepared planar chiral nanostructures.[44] Here, we show that this concept is also applicable for the characterization of single chiral plasmonic molecules by analyzing the influence of structural defects on the chiral optical response. We find that even minute structural differences lead to significant changes in the chiral optical response which underlines once again the unique ability of chiral plasmonic structures to encode their 3D conformation into optical scattering spectra.

At this point, we must stress an important difference between our plasmonic system and solutions of chiral molecules. The top-down fabrication of plasmonic nanostructures leads to a structural ordering of the resulting chiral plasmonic molecules which is ultimately induced by the surface on which they are fabricated. Depending on the arrangement of the individual nanostructures the overall arrangement can be biaxial. Consequently, the intrinsic chiral response of the nanostructures might be masked and overlaid by linear birefringence. In many experimental studies on chiral plasmonic systems, the structures have thus been arranged in, for example, a C_4 symmetric lattice.[29,45–47] Such an arrangement renders the overall structures uniaxial and thus suppresses linear birefringence. It is interesting to note, however, that the underlying biaxiality is in fact due to the individual nanostructure. Every individual chiral nanostructure exhibits distinct scattering properties for excitation with different linearly polarized incident light, thus being biaxial or even triaxial (when taking all three dimensions into account).[26,48] The suppression of in-plane polarization conversion in a lattice arrangement is therefore in fact realized by creating a C_4 symmetric unit cell. For obvious reasons, such an effect cannot be observed in solutions of molecules. Here, the orientation is purely random and the measured CD response is solely caused by the chiral properties of the molecules.

Interestingly, even for a single chiral molecule on an interface, the orientation will play an important role and it will most probably not be possible to measure the CD response of such a single molecule. As soon as one immobilizes a chiral structure on an interface, the different optical properties of the molecule under excitation along the distinct molecular axes will cause additional contributions to the signal.[26] However, as mentioned, an arrangement of chiral structures can be rendered uniaxial. For single chiral structure investigations, it is indispensable to take these effects into account. The most straightforward way is to suppress linear birefringence in creating a C_4 symmetric cell consisting of four chiral molecules or subgroups.

2. Results and Discussions

The enantiomers of our single plasmonic oligomer are shown in **Figure 1**a. They consist of four chiral quadrumers rotated by 90° with respect to each other.[46] This arrangement renders the single oligomer uniaxial and thus suppresses the aforementioned contributions due to polarization conversions, as discussed above. A quadrumer—the fundamental building block—consists of three gold disks in the first (lower) layer and

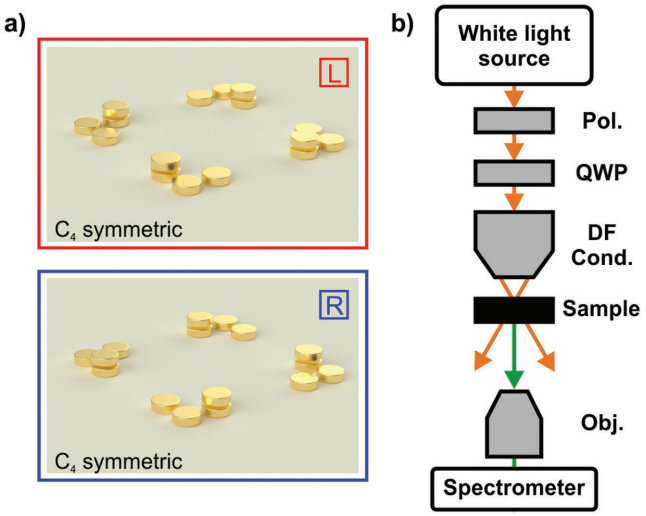

Figure 1. a) Schematic representation of the enantiomers of a single plasmonic oligomer in C_4 symmetry. The left-handed structure is shown in the upper picture and is marked in red, whereas the right-handed structure is shown in the lower picture and is marked in blue. The oligomer consists of four identical chiral quadrumers rotated by 90° with respect to each other. b) Sketch of the measurement setup. Light from a high-intensity white light source passes through a polarizer and a quarter wave plate (QWP) to create left-circularly polarized (LCP) and right-circularly polarized (RCP) light. A dark-field condenser is used for illumination, the objective collects only scattered light which is sent into a spectrometer.

one gold disk in the second (upper) layer. The diameter of all disks is 100 nm. The position of the upper disk can easily be changed to obtain the two enantiomers as well as the achiral oligomer. The structures are fabricated by standard two-layer electron beam lithography. First, a 70 nm thick dielectric layer (PC403, JCR) is spin-coated on a glass substrate (1×1 cm^2). Afterward, a two-layer positive tone resist system (poly(methyl) methacrylate, 200K and 950K, Allresist) is spin-coated followed by electron beam exposure (Raith eLine Plus) to define the first layer of the single oligomers. After development, a 3 nm Cr adhesion layer and a 40 nm gold layer are deposited by electron beam evaporation. After a lift-off process in a commercial n-ethyl-2-pyrrolidon (NEP)-based remover (Allresist), another 70 nm thick dielectric layer is spin-coated. The second layer is fabricated in a subsequently aligned electron beam lithography step, followed by development, Cr and Au evaporation, lift-off, and a final spin-coating of a 70 nm dielectric layer to end up with a fully embedded gold structure. The distance between neighboring single oligomers is 8 µm.

A modified dark-field transmission microscope (Nikon Eclipse TE2000-U) combined with a grating spectrograph (Princeton Instruments SP2500i) and a Peltier-cooled front-illuminated CCD camera (Acton PIXIS 256E) is used to resolve a single oligomer and to measure its scattering spectrum in the visible and near-infrared spectral range (500–1000 nm). The spectroscopy setup is schematically shown in Figure 1b.[49] Light from a high-intensity laser-driven plasma white light source (Energetiq EQ-99) passes through a polarizer (Thorlabs LPVIS100) and a broadband quarter wave plate (B. Halle RAC 5.4.20) to obtain left-circularly polarized (LCP) and right-circularly polarized (RCP) light. A dark-field condenser (NA

= 0.8–0.95) cuts out the center cone of the primary beam and focuses the light onto the sample. The positioning of the single oligomers in focus is performed with a high precision stage (Märzhäuser SCAN IM 120 × 10). Due to the high NA of the condenser and the resulting high angle of incidence, the primary light passes the objective (magnification 60×) and only the scattered light from a single oligomer is guided into the spectrometer. The exposure time for each measurement of a single oligomer is t_{exp} = 4 s. As a reference, we measure the LCP and RCP scattering spectrum of a chemically roughened silica substrate, which is assumed to give an isotropic and spectrally flat optical response. Background correction is performed by taking the average of ten dark measurements, when the entrance slit of the spectrometer is closed and subtracting the resulting averaged individual pixel intensity from each measurement.

Figure 2 shows the dark-field scattering signal in transmission of two exemplary single oligomers for circularly polarized excitation. One left- and one right-handed single plasmonic oligomer is illuminated with incident LCP (dashed) and RCP light (solid). The spectra of the L-enantiomer are plotted in red, the ones of the R-enantiomer in blue. The resonance position of the left-handed oligomer is blueshifted by $\Delta\lambda \approx 30$ nm. This effect is observed for all structures measured in this work. Due to the small size of the nanoparticles, the energetic splitting between the coupled modes of the oligomers is strongly reduced as compared to the near-infrared wavelength range and thus the spectral signatures of these modes are no longer well separated. This fact manifests itself in the "close-to-single-peak" appearance of the scattering spectrum. For both enantiomers, we observe clear differences for LCP and RCP excitation in the wavelength region from λ = 650 nm to λ = 800 nm. For comparison, the scattering spectra of the achiral structure are plotted in Figure S1 (Supporting Information). Furthermore, Figure 2 depicts tilted scanning electron microscope (SEM) images of the two-layered left- and right-handed single oligomers, demonstrating excellent structural control.

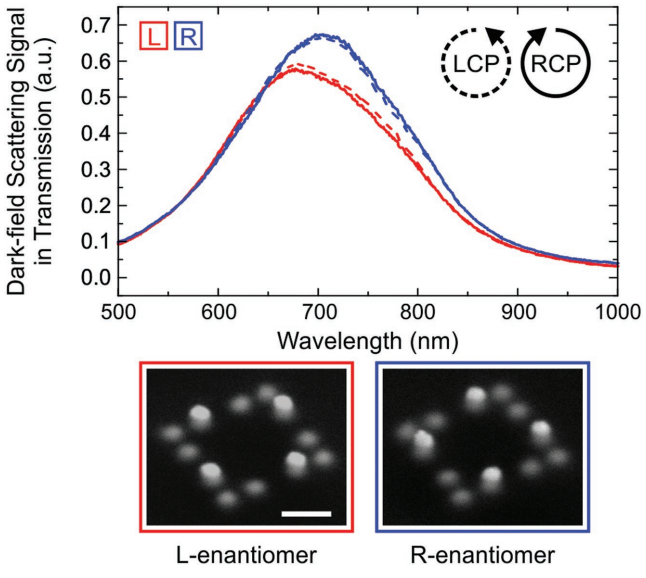

Figure 2. Scattering spectra of single plasmonic oligomers in C_4 symmetry, illuminated with LCP (dashed) and RCP light (solid). The resonance position of the L-structure (red) is blueshifted by $\Delta\lambda$ = 30 nm in comparison to the R-structure (blue). The typical interchanging effect from RCP to LCP light is clearly observed. In addition, tilted scanning electron microscope (SEM) images of both enantiomers are shown (30° tilting angle). The scale bar is 200 nm and valid for both images.

In molecular physics or molecular chemistry, CD is defined as the difference in absorption of LCP and RCP light, namely, as CD = $A_{LCP} - A_{RCP}$. In our case, however, we are defining the chiroptical measurement signal via scattering, that is, as the difference of the scattering spectra measured with incident RCP and LCP light, namely, $S_{RCP} - S_{LCP}$ (this definition is arbitrary with respect to the sign). Characterizing a chiroptical response via differential scattering appears counterintuitive at first sight. However, it needs to be stressed that molecular systems and plasmonic systems are very different with respect to their interaction with light. Due to their small size compared to the wavelength of light, molecules do only absorb light and virtually no scattering can be observed. The difference in transmission is thus fully determined by the difference in absorption (apart from a sign change). Plasmonic molecules on the other hand absorb and scatter light. In fact, we can thus envision two distinct contributions in the chiroptical response of plasmonic structures.[50] One is related to absorption, one to scattering. It has in fact been shown that even without near-field coupling a purely scattering type chiroptical response can be observed.[51] This behavior suggests that the chiroptical response of plasmonic structures is much richer than it is for molecules. In any case, it underlines that our definition of the measurement signal in this experimental study is reasonable as absorption and scattering are known to contribute. Thus, we expect to only measure part of the chiral response and that absorption spectroscopy, which can also be performed on a single nanostructure level, might reveal additional information and insight.[52–54] Please note that we define the differential scattering as $S_{RCP} - S_{LCP}$, whereas CD is $A_{LCP} - A_{RCP}$. We choose this difference in sign arbitrary. Nevertheless, we link this definition to the relation between the absorption and scattering cross section, which both contribute to the extinction cross section as $\sigma_{ext} = \sigma_{abs} + \sigma_{scat}$.

We plot in **Figure 3** the differential scattering of 2 × 18 single oligomers (18 left-handed and 18 right-handed structures). The spectra are obtained by taking the difference between the individual scattering spectra for RCP and LCP light ($S_{RCP} - S_{LCP}$). The left panel shows the chiroptical response of 18 left-handed single oligomers plotted in red and the right panel the chiroptical response of all 18 right-handed single oligomers plotted in blue. We sorted the spectra in a waterfall plot depending on their spectral motifs. Starting at the top with spectra where the left feature at $\lambda \approx 680$ nm is very pronounced, followed by spectra where we observe two clearly distinguishable features, we end up with spectra with a distinct feature at $\lambda \approx 780$ nm. All 2 × 18 structures are fabricated with nominally identical parameters on the same sample. We clearly show that even these nominally identical structures of each handedness show considerably different chiral spectral features, which we ascribe to minute structural differences due to fabricational tolerances. However, the overall trend between all spectra of structures with the same handedness is the same. Interestingly, despite the significant structural differences between all particles we find pairs of left- and right-handed single oligomers which

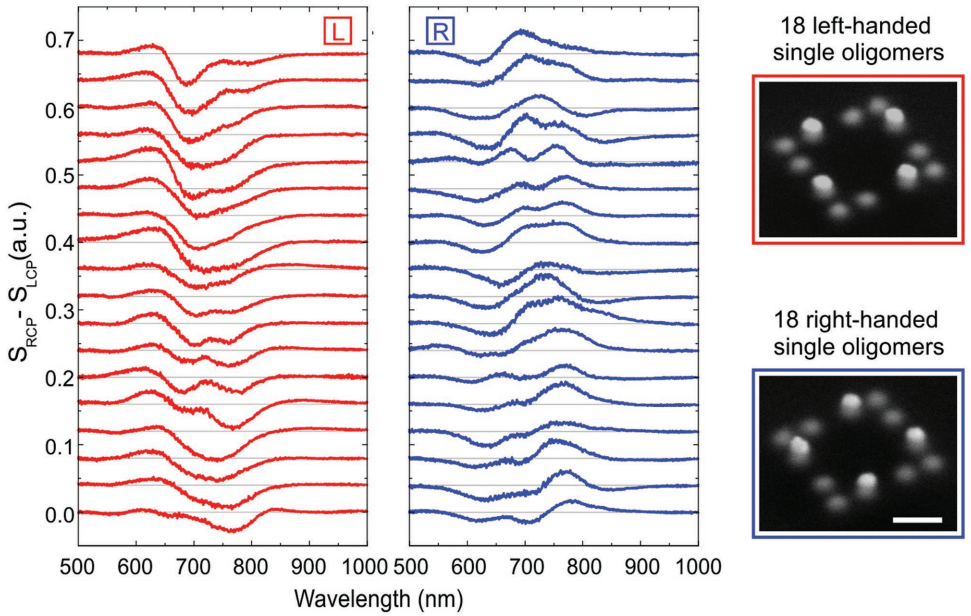

Figure 3. Differential scattering ($S_{RCP} - S_{LCP}$) spectra of 2 × 18 single oligomers (18 left-handed and 18 right-handed). Left-handed structures are marked in red and right-handed structures in blue. We sorted the spectra depending on their spectral features. The offset between the spectra is 0.04 in arbitrary units. Although all oligomers are fabricated with nominally identical parameters, we observe distinct differences in the chiroptical behavior. Exemplarily, SEM pictures are shown for both enantiomers. The scale bar in the SEM images is 200 nm and valid for both images.

possess mirror symmetric chiroptical responses. This indicates that their deviations from the ideal structure are similar such that they are mirror symmetric, that is, true enantiomers. To further analyze this behavior, we show the chiroptical response of three such pairs in **Figure 4**.

The measurements depicted in Figure 4 demonstrate that it is indeed possible to measure the differential scattering signal of single right- and left-handed structures that exhibit a clean inversion of the signal when changing the handedness. Overall, we observe a rich set of spectral signatures and excellent mirror

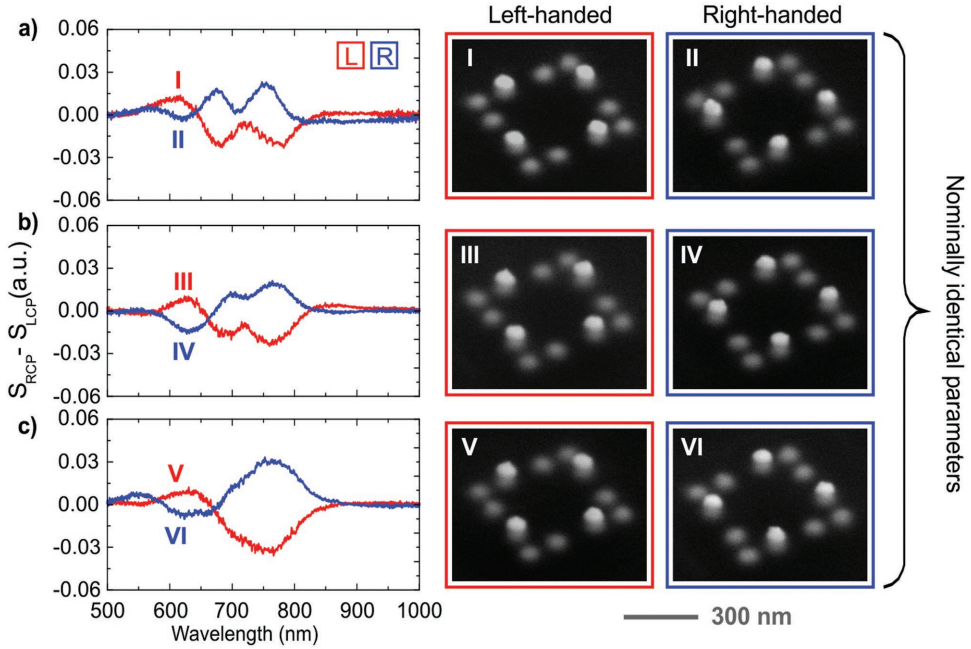

Figure 4. Differential scattering ($S_{RCP} - S_{LCP}$) spectra of 2 × 3 single oligomers with nominally identical parameters (three left-handed and three right-handed) selected from the measurements shown in Figure 3. The spectra of each oligomer and the corresponding SEM images are enumerated from I to VI for clarity. Left-handed oligomers are plotted and marked in red and right-handed oligomers in blue. Despite identical fabrication we observe distinct differences between these spectra. Correlating the spectra with the corresponding SEM images does not help to unravel the structural cause for these differences, underpinning the unique ability of chiral structures to spectrally encode their 3D conformation.

symmetric behavior, as would be expected for enantiomers in first place. The oligomers in Figure 4a exhibit two clearly separated features. These features are also observed in the differential scattering signal of the oligomers measured in Figure 4b, however they are not as pronounced and well separated. The two enantiomers in Figure 4c show only a single feature in this wavelength region. It is more an envelope of the double peak feature. In principle, this behavior is very surprising. Once more, we emphasize that *all* enantiomers of Figure 4 had the same nominal parameters.

As mentioned above, the chiroptical response of plasmonic structures is strongly dependent on *their exact* conformation. While electron beam fabrication is an extremely precise technique, the small sizes of the particles and the double-layer nature of the structures make fabrication challenging and slightest differences in the relative arrangement and shape of the particles are to be expected. We can thus suspect these minute differences to cause the distinct spectral features.[55] To investigate this correlation, we performed high-resolution correlative SEM investigations. The right column of Figure 4 depicts SEM images of the selected oligomer pairs. In addition, SEM images of the same oligomers taken at normal incidence are shown in Figure S2 (Supporting Information). Even a close inspection of the SEM images does not reveal *any* traceable structural differences. While a few particles seem to be of slightly different shape and minutely shifted in position, it is not possible to assign any of the observed spectral differences to a distinct structural one. We can thus *not* infer from the high-resolution microscopy investigation on the origin of the spectral differences. Even though we have a very high degree of structural control in utilizing high-resolution electron beam lithography, the accuracy is not high enough to warrant for the fabrication of *truly identical* structures. This observation once again underpins the unique ability of chiral structures to encode 3D arrangements which are below the resolution limit of our SEM investigations. Additionally, it stresses the importance of all structural deviations in the fabrication of chiral nanostructures, for top-down as well as bottom-up self-assembled nanosystems, in particular as soon as they deform or order on surfaces.

The spectral signatures in the differential scattering are caused by distinct plasmonic modes. It is therefore intriguing to try and track the differences in the optical response and thus the differences in structural arrangement by analyzing the plasmonic mode formation in the oligomers. However, it needs to be stressed that the mode formation is highly complex. Each individual quadrumer consists of four particles with two in-plane energetically degenerate dipolar modes. These result in a total of eight coupled modes (disregarding the higher order quadrupolar modes of the disks). Many of these modes do not have a distinct handedness and will thus be excited similarly by RCP and LCP incident light. The overall chiroptical response will be highly complex and modal signatures will also spectrally overlap. It is thus not straightforwardly possible to assign a certain spectral signature to a certain plasmonic mode. In well-designed structures, such as the plasmonic Born–Kuhn model[56,57] which consists of two edge-stacked single nanorods with one dipolar mode each, the spectral features can unambiguously be assigned and spectral changes can thus be assigned to structural ones. In our more complex system, this is not straightforwardly possible.

Until now, we have shown only the influence of structural defects onto the chiroptical response of the left- and right-handed enantiomers. In addition, it is easy to define the achiral version by changing the position of the disks in the upper layer as seen in the SEM images in **Figure 5**. This results in an unhanded C_4 symmetric single oligomer. Figure 5 shows the differential scattering of two achiral single oligomers fabricated with nominally identical parameters. Both structures do exhibit a chiroptical response, despite the fact they are designed to be achiral. However, it is well known from previous studies that minute deviations from the ideal achiral arrangement lead to detectable chiroptical responses.[21,46] We can clearly observe this effect in the spectra shown in Figure 5: The single oligomer in Figure 5a, colored in dark brown with the corresponding SEM image, exhibits a differential scattering spectrum which exhibits features of the L-enantiomers, as shown in Figure 3. The single oligomer in Figure 5b, colored in light brown with the corresponding SEM image, possesses a differential scattering spectrum with features of the R-enantiomer.

Our findings appear somewhat unexpected as such strong deviations in the chiral optical response have not been observed in array measurements, even though structural imperfections should have an equally strong influence here. The main difference is, of course, related to ensemble averaging. One of the main advantages of our technique is the ability to study *individual* chiral oligomers and thus eliminate all averaging effects.

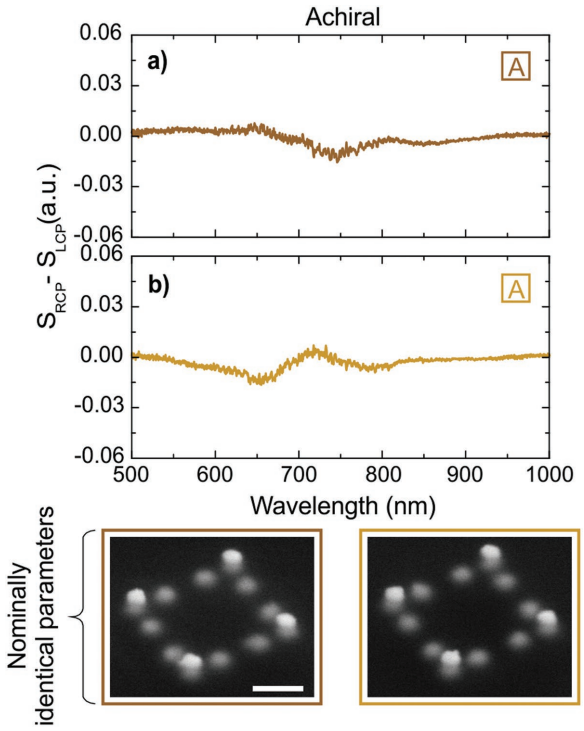

Figure 5. Differential scattering spectra and corresponding SEM images for two achiral single oligomers. a) The chiroptical response of the oligomer is reminiscent of the behavior of the L-enantiomers in Figure 3, whereas the oligomer in b) shows features of the R-enantiomers. The cause for this behavior lies with inaccuracies and limitations in the fabrication process which leads to misalignments and to deviations from the perfect disk shape. The scale bar is 200 nm.

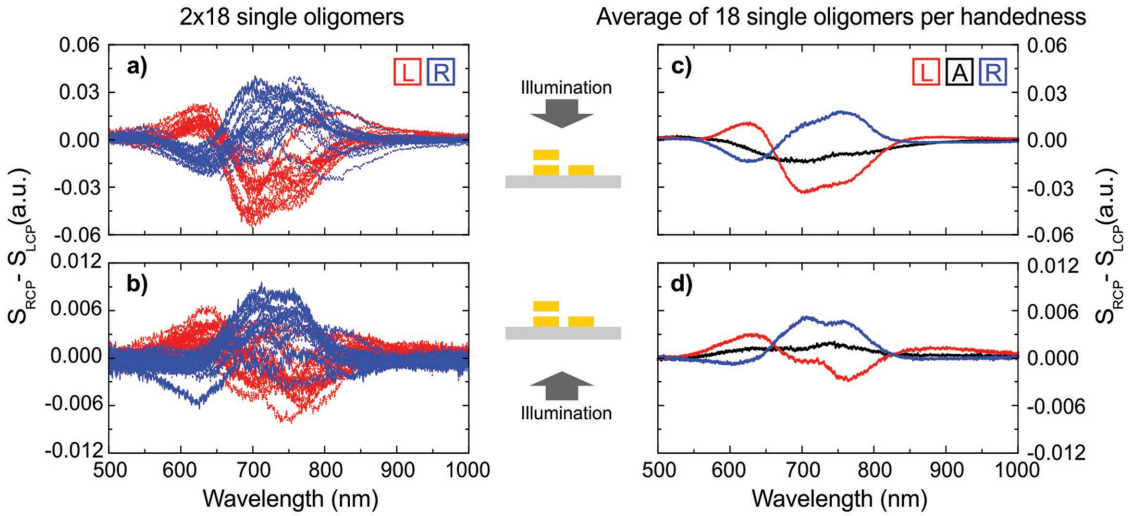

Figure 6. a) Differential scattering of 2 × 18 oligomers (18 left- and 18 right-handed ones) measured in forward illumination. While we observe distinct variations, the overall trend for all structures is very similar. b) Corresponding differential scattering for the 36 oligomers measured in backward illumination. We observe a larger spread in the chiroptical response, yet, overall the trend is very similar as in panel (a). c,d) The averaged scattering difference of the 18 single oligomers per handedness shown in panels (a) and (b) in forward and backward illumination, respectively, as well as of 18 achiral ones. We observe mirror symmetric differential scattering spectra for both illumination directions. The chiroptical response of the achiral structure is almost zero and shows only small deflections.

In order to demonstrate this, we have again plotted the differential scattering spectra of all 2 × 18 oligomers in **Figure 6**a. We see distinct differences between the spectra, as discussed in Figure 3. However, the overall trend of all structures with the same structural handedness is the same. One can create an artificial ensemble average by summing the contribution of all oligomers up and plotting the average response. This response, also for a set of 18 achiral structures, is shown in Figure 6c. The spectra display good mirror symmetry, and the averaged spectrum of the achiral structures shows barely any chiroptical signal, as would be expected. However, we explain these minimal differential scattering signals with the minute structural differences. It is obvious that it is not possible to fabricate a "perfect" achiral structure. Therefore, all achiral oligomers possess either left- or right-handed properties. The sign of the averaged achiral signal indicates that there are more slightly left-handed achiral single oligomers.

We can perform another important consistency check. Illuminating the structures from the back side should result in a similar chiroptical response. While the exact mode structure is not expected to be reproduced, the overall trend, that is, the handedness, must not change. Figure 6b depicts the differential scattering spectra of the 2 × 18 oligomers shown in Figure 6a for backward illumination. We again observe differences between the spectra, yet, the overall trend for oligomers of the same handedness is similar and comparable to the results in Figure 6a. The spectra show a larger spread which can be explained by the illumination geometry. For backward illumination, the focused light beam passes through the glass substrate first. Due to refraction, we end up with slightly different angles of incidence, which has already an influence on the dark-field scattering spectrum of a single oligomer. Furthermore, it is more difficult to place the respective single oligomer in focus because it appears blurrier due to the substrate "on top." Figure 6d again shows the average differential scattering of the 2 × 18 oligomers and the 18 achiral ones. We see excellent mirror symmetry and the same mode structure and position as observed for forward illumination. The achiral averaged differential scattering signal is again close to zero but changes its sign. This is explained with the different angle of incidence due to refraction in backward illumination which changes the "field of view" and therefore the arrangement of the achiral oligomers with respect to incident light beam. Thus, the minute structural differences lead to the inverted averaged differential scattering signal of the 18 achiral oligomers when changing the illumination direction.

These measurements clearly prove that we are indeed measuring the chiroptical response of single chiral plasmonic oligomers which are consistent with the expected behavior and with previously performed array measurements. To underline these findings, we also performed array measurements, which are shown in the Supporting Information. When utilizing our experimental setup in transmission bright-field hyperspectral imaging mode we can measure the chiroptical response of sections of the array of varying sector size. When scanning the measurement window over the array we also observe distinct changes in the chiroptical response which are normally masked by ensemble averaging in the entire array, as shown in Figures S3 and S4 (Supporting Information).

Finally, as mentioned, all our structures are C_4 symmetric in order to remove any contributions of polarization conversion to the chiroptical response. To stress the importance of such an arrangement, we show in Figure S5 (Supporting Information) the differential scattering of 2 × 2 C_1 symmetric single oligomers (two left- and two right-handed) in forward and backward illumination. The spectra show no clear trend of mirroring between right- and left-handed structures, demonstrating that polarization conversion can lead to virtually any differential scattering signal depending on minor fabrication differences.

3. Conclusions

In conclusion, we have demonstrated that we can measure reproducibly the chiroptical response of single plasmonic oligomers in the visible spectral range. The chiroptical response of such single oligomers strongly depends on the precise structural arrangement as well as structural defects. Minute structural differences manifest themselves as distinct differences in the differential scattering signal. However, it is not possible to relate the differences in the chiroptical response to clear differences in the structural alignment and shape, or vice versa. Similar to the averaging effect in a periodically arranged array, we obtained mirror symmetric differential scattering spectra for left- and right-handed single oligomers and almost no chiroptical response for the achiral oligomer, which also holds for backward illumination. Our measurements underpin the unique ability of chiral plasmonic structures to encode their conformation into chiroptical spectra. Even when utilizing high-resolution electron beam lithography, the inherent structural control does not suffice to ensure identical structures. These findings have immediate implications for other fabrication techniques, such as self-assembly. Here, due to the polydispersity in nanoparticle size and shape, one expects an even larger spread in the exact conformation of the fabricated structures. This issue becomes even more pressing as soon as the structures are immobilized on an interface and slightly deform. Our work could find applications in the fabrication, optimization, and measurement of single plasmonic particles but might also be important toward single chiral object sensing.

Supporting Information

Supporting Information is available from the Wiley Online Library or from the author.

Acknowledgements

The authors acknowledge financial support from the European Research Council (ERC Advanced Grant Complexplas), Bundesministerium für Bildung und Forschung, Deutsche Forschungsgemeinschaft (SPP1839 Tailored Disorder and SPP1391 Ultrafast Nanooptics), and Baden-Württemberg Stiftung. The authors thank EU COST MP1302 (Nanospectroscopy) for support of a workshop on chiral nanophotonics which initiated the compilation of this paper. The authors would like to thank Florian Sterl for his contributions to the experimental setup. Xiaoyang Duan and Laura Na Liu are acknowledged for assistance in an early stage of the experiment.

Conflict of Interest

The authors declare no conflict of interest.

Keywords

chirality, circular dichroism spectroscopy, dark-field spectroscopy, single plasmonic particle

Received: January 23, 2018
Revised: March 23, 2018
Published online: May 9, 2018

[1] N. Berova, K. Nakanishi, R. W. Woody, *Circular Dichroism: Principles and Applications*, Wiley-VCH, New York **2000**.
[2] H. K. Bisoyi, Q. Li, *Angew. Chem., Int. Ed.* **2016**, *55*, 2994.
[3] L. D. Barron, *Molecular Light Scattering and Optical Activity*, Cambridge University Press, Cambridge, UK **2004**.
[4] G. D. Fasman, *Circular Dichroism and the Conformational Analysis of Biomolecules*, Springer US, New York **1996**.
[5] Y. Zhao, M. A. Belkin, A. Alù, *Nat. Commun.* **2012**, *3*, 1877.
[6] K. M. McPeak, C. D. Van Engers, M. Blome, J. H. Park, S. Burger, M. A. Gosálvez, A. Faridi, Y. R. Ries, A. Sahu, D. J. Norris, *Nano Lett.* **2014**, *14*, 2934.
[7] K. M. McPeak, C. D. Van Engers, S. Bianchi, A. Rossinelli, L. V. Poulikakos, L. Bernard, S. Herrmann, D. K. Kim, S. Burger, M. Blome, S. V. Jayanti, D. J. Norris, *Adv. Mater.* **2015**, *27*, 6244.
[8] V. K. Valev, J. J. Baumberg, C. Sibilia, T. Verbiest, *Adv. Mater.* **2013**, *25*, 2517.
[9] J. G. Gibbs, A. G. Mark, S. Eslami, P. Fischer, *Appl. Phys. Lett.* **2013**, *103*, 98.
[10] A. G. Mark, J. G. Gibbs, T. C. Lee, P. Fischer, *Nat. Mater.* **2013**, *12*, 802.
[11] R. Quidant, M. Kreuzer, *Nat. Nanotechnol.* **2010**, *5*, 762.
[12] Y. Zhao, A. A. E. Saleh, J. A. Dionne, *ACS Photonics* **2016**, *3*, 304.
[13] J. K. Gansel, M. Latzel, A. Frölich, J. Kaschke, M. Thiel, M. Wegener, *Appl. Phys. Lett.* **2012**, *100*, 2010.
[14] J. K. Gansel, M. Thiel, M. S. Rill, M. Decker, K. Bade, V. Saile, G. von Freymann, S. Linden, M. Wegener, *Science* **2009**, *325*, 1513.
[15] J. Kaschke, M. Wegener, *Opt. Lett.* **2015**, *40*, 3986.
[16] A. Kuzyk, R. Schreiber, Z. Fan, G. Pardatscher, E. M. Roller, A. Högele, F. C. Simmel, A. O. Govorov, T. Liedl, *Nature* **2012**, *483*, 311.
[17] W. Yan, L. Xu, C. Xu, W. Ma, H. Kuang, L. Wang, N. A. Kotov, *J. Am. Chem. Soc.* **2012**, *134*, 15114.
[18] M. J. Urban, P. K. Dutta, P. Wang, X. Duan, X. Shen, B. Ding, Y. Ke, N. Liu, *J. Am. Chem. Soc.* **2016**, *138*, 5495.
[19] A. J. Mastroianni, S. Claridge, A. P. Alivisatos, *J. Am. Chem. Soc.* **2010**, *131*, 8455.
[20] W. Chen, A. Bian, A. Agarwal, L. Liu, H. Shen, L. Wang, C. Xu, N. A. Kotov, *Nano Lett.* **2009**, *9*, 2153.
[21] V. E. Ferry, J. M. Smith, A. P. Alivisatos, *ACS Photonics* **2014**, *1*, 1189.
[22] Z. Fan, A. O. Govorov, *Nano Lett.* **2010**, *10*, 2580.
[23] C. Song, M. G. Blaber, G. Zhao, P. Zhang, H. C. Fry, G. C. Schatz, N. L. Rosi, *Nano Lett.* **2013**, *13*, 3256.
[24] A. Guerrero-Martínez, B. Auguié, J. L. Alonso-Gómez, Z. Džolić, S. Gómez-Graña, M. Žinić, M. M. Cid, L. M. Liz-Marzán, *Angew. Chem., Int. Ed.* **2011**, *50*, 5499.
[25] X. Shen, P. Zhan, A. Kuzyk, Q. Liu, A. Asenjo-Garcia, H. Zhang, F. J. García de Abajo, A. Govorov, B. Ding, N. Liu, *Nanoscale* **2014**, *6*, 2077.
[26] R. Schreiber, N. Luong, Z. Fan, A. Kuzyk, P. C. Nickels, T. Zhang, D. M. Smith, B. Yurke, W. Kuang, A. O. Govorov, T. Liedl, *Nat. Commun.* **2013**, *4*, 3948.
[27] A. Kuzyk, R. Schreiber, H. Zhang, A. O. Govorov, T. Liedl, N. Liu, *Nat. Mater.* **2014**, *13*, 862.
[28] C. Zhou, X. Duan, N. Liu, *Nat. Commun.* **2015**, *6*, 1.
[29] M. Hentschel, V. E. Ferry, A. P. Alivisatos, *ACS Photonics* **2015**, *2*, 1253.
[30] B. Frank, X. Yin, M. Schäferling, J. Zhao, S. M. Hein, P. V. Braun, H. Giessen, *ACS Nano* **2013**, *7*, 6321.
[31] M. L. Nesterov, X. Yin, M. Schäferling, H. Giessen, T. Weiss, *ACS Photonics* **2016**, *3*, 578.
[32] Z. Xu, L. Xu, Y. Zhu, W. Ma, H. Kuang, L. Wang, C. Xu, *Chem. Commun.* **2012**, *48*, 5760.
[33] A. O. Govorov, Z. Fan, P. Hernandez, J. M. Slocik, R. R. Naik, *Nano Lett.* **2010**, *10*, 1374.

[34] M. Hentschel, M. Schäferling, X. Duan, H. Giessen, N. Liu, *Sci. Adv.* **2017**, *3*, e1602735.
[35] A. O. Govorov, Y. K. Gun'ko, J. M. Slocik, V. A. Gérard, Z. Fan, R. R. Naik, *J. Mater. Chem.* **2011**, *21*, 16806.
[36] A. Ben-Moshe, B. M. Maoz, A. O. Govorov, G. Markovich, *Chem. Soc. Rev.* **2013**, *42*, 7028.
[37] P. Banzer, P. Woźniak, U. Mick, I. De Leon, R. W. Boyd, *Nat. Commun.* **2016**, *7*, 13117.
[38] Y. Hwang, B. Hopkins, D. Wang, A. Mitchell, T. J. Davis, J. Lin, X. C. Yuan, *Laser Photonics Rev.* **2017**, *1*, 1700216.
[39] G. J. Nusz, S. M. Marinakos, A. C. Curry, A. Dahlin, F. Hook, A. Wax, A. Chilkoti, *Anal. Chem.* **2008**, *80*, 984.
[40] L. S. Slaughter, W. S. Chang, P. Swanglap, A. Tcherniak, B. P. Khanal, E. R. Zubarev, S. Link, *J. Phys. Chem. C* **2010**, *114*, 4934.
[41] X. Lu, J. Wu, Q. Zhu, J. Zhao, Q. Wang, L. Zhan, W. Ni, *Nanoscale* **2014**, *6*, 14244.
[42] L. Y. Wang, K. W. Smith, S. Dominguez-Medina, N. Moody, J. M. Olson, H. Zhang, W. S. Chang, N. Kotov, S. Link, *ACS Photonics* **2015**, *2*, 1602.
[43] W. Ma, H. Kuang, L. Wang, L. Xu, W.-S. Chang, H. Zhang, M. Sun, Y. Zhu, Y. Zhao, L. Liu, C. Xu, S. Link, N. A. Kotov, *Sci. Rep.* **2013**, *3*, 1934.
[44] S. Zu, Y. Bao, Z. Fang, *Nanoscale* **2016**, *8*, 3900.
[45] M. Decker, R. Zhao, C. M. Soukoulis, S. Linden, M. Wegener, *Opt. Lett.* **2010**, *35*, 1593.
[46] M. Hentschel, M. Schäferling, T. Weiss, N. Liu, H. Giessen, *Nano Lett.* **2012**, *12*, 2542.
[47] J. Kaschke, J. K. Gansel, M. Wegener, *Opt. Express* **2012**, *20*, 26012.
[48] E. Efrati, W. T. M. Irvine, *Phys. Rev. X* **2014**, *4*, 1.
[49] A. Tittl, X. Yin, H. Giessen, X. D. Tian, Z. Q. Tian, C. Kremers, D. N. Chigrin, N. Liu, *Nano Lett.* **2013**, *13*, 1816.
[50] B. Hopkins, A. N. Poddubny, A. E. Miroshnichenko, Y. S. Kivshar, *Laser Photonics Rev.* **2016**, *10*, 137.
[51] V. E. Ferry, M. Hentschel, A. P. Alivisatos, *Nano Lett.* **2015**, *15*, 8336.
[52] M. A. van Dijk, A. L. Tchebotareva, M. Orrit, M. Lippitz, S. Berciaud, D. Lasne, L. Cognet, B. Lounis, *Phys. Chem. Chem. Phys.* **2006**, *8*, 3486.
[53] M. Husnik, S. Linden, R. Diehl, J. Niegemann, K. Busch, M. Wegener, *Phys. Rev. Lett.* **2012**, *109*, 1.
[54] O. L. Muskens, N. Del Fatti, F. Vallée, J. R. Huntzinger, P. Billaud, M. Broyer, *Appl. Phys. Lett.* **2006**, *88*, 63109.
[55] N. Liu, M. Hentschel, T. Weiss, A. P. Alivisatos, H. Giessen, *Science* **2011**, *332*, 1407.
[56] X. Yin, M. Schäferling, B. Metzger, H. Giessen, *Nano Lett.* **2013**, *13*, 6238.
[57] B. Auguié, J. L. Alonso-Gómez, A. Guerrero-Martínez, L. M. Liz-Marzán, *J. Phys. Chem. Lett.* **2011**, *2*, 846.